



HAL
open science

Angular Velocity Nonlinear Observer From Single Vector Measurements

Lionel Magnis, Nicolas Petit

► **To cite this version:**

Lionel Magnis, Nicolas Petit. Angular Velocity Nonlinear Observer From Single Vector Measurements. IEEE Transactions on Automatic Control, 2016, 61 (9), pp.2473-2483. 10.1109/TAC.2015.2501358 . hal-01369515

HAL Id: hal-01369515

<https://minesparis-psl.hal.science/hal-01369515>

Submitted on 21 Sep 2016

HAL is a multi-disciplinary open access archive for the deposit and dissemination of scientific research documents, whether they are published or not. The documents may come from teaching and research institutions in France or abroad, or from public or private research centers.

L'archive ouverte pluridisciplinaire **HAL**, est destinée au dépôt et à la diffusion de documents scientifiques de niveau recherche, publiés ou non, émanant des établissements d'enseignement et de recherche français ou étrangers, des laboratoires publics ou privés.

Angular velocity nonlinear observer from single vector measurements

Lionel Magnis, Nicolas Petit

Index Terms

Sensor and data fusion; nonlinear observer and filter design; time-varying systems; guidance navigation and control.

Abstract

The paper proposes a technique to estimate the angular velocity of a rigid body from single vector measurements. Compared to the approaches presented in the literature, it does not use attitude information nor rate gyros as inputs. Instead, vector measurements are directly filtered through a nonlinear observer estimating the angular velocity. Convergence is established using a detailed analysis of a linear-time varying dynamics appearing in the estimation error equation. This equation stems from the classic Euler equations and measurement equations. As is proven, the case of free-rotation allows one to relax the persistence of excitation assumption. Simulation results are provided to illustrate the method.

I. INTRODUCTION

This article considers the question of estimating the angular velocity of a rigid body from signals from embedded sensors. This general question is of particular importance in various fields of engineering, and in particular for the problem of orientation control, as shown in numerous applications [1], [2], [3], [4] for spacecraft, unmanned aerial vehicles, guided ammunitions, to name a few.

In the literature, two types of methods have been proposed to address this question. First, one can directly measure the angular velocity by using a specific sensor. This straightforward solution requires a strap-down rate gyro [5]. However, gyros have numerous drawbacks. They are very expensive compared to direction sensors, prone to saturation during high rate rotations [6] and subject to failure. A famous example is the Hubble Space Telescope, which was put into “safe hold” (i.e. sleep mode) on November 13rd, 1999 as four of its six gyros malfunctioned [7]. Eventually, the six gyros were replaced in 1999 and again in 2009 during the highly expensive missions STS-103 and STS-125 [8].

Fortunately, gyros are not strictly necessary in the applications considered here. A recent trend is to replace (or consolidate) the gyro measurements with other sensors. In particular, vector measurements have been investigated for estimating ω for the last 15 years. An example of this “gyro-less” trend is the Solar Anomalous and Magnetospheric Particle Explorer (SAMPEX) spacecraft, which was launched in July 1992 and whose inertial unit only comprises Sun sensors and magnetometers [9]. The alternative to gyros is a *two-step* approach. In the first step, attitude is determined from measurements of known reference vectors. Then, in the second step, attitude variations are used to estimate the angular velocity.

The first step is detailed in [10]. In a nutshell, when two independent vectors are measured with vector sensors attached to a rigid body, the attitude of the rigid body can be found under the form the solution of the Wahba problem [11] which is a minimization problem having as unknown the rotation matrix from a fixed frame to the body frame. Thus, at any instant, full attitude information can be obtained [12], [13], [14], [15]. In principle, this is sufficient to perform the second step: once the attitude is known, angular velocity can be estimated from a time-differentiation. However, noise disturbs this process. To address this issue, introducing *a priori* information in the estimation process allows one to filter-out noise from the estimates. Following this approach, numerous observers based on the Euler equations have been proposed to estimate angular velocity from full attitude information [1], [16], [17], [18].

Besides this two-step approach, which requires measurements of two independent reference vectors, a more direct and less requiring solution can be proposed. In this paper, we expose an algorithm that directly uses the measurements of a *single* vector and reconstructs the angular velocity in a simple manner, by means of a nonlinear observer. This is the contribution of this article. In a related philosophy, we have recently proposed an observer using the measurements from two linearly independent vectors as input [19]. The present paper studies a similarly structured observer. However, due to the fact that here only a single vector measurement is employed, the arguments of proof are completely different, and result in a new and independent contribution.

The paper is organized as follows. In Section II, we introduce the notations and the problem statement. We analyze the attitude dynamics (rotation and Euler equations) and relate it to the measurements. In Section III, we define the proposed nonlinear observer. The observer has an extended state and uses output injection. To prove its convergence, the error equation is identified as a linear time-varying (LTV) system perturbed by a linear-quadratic term. Under a persistent excitation (PE) assumption, the LTV dynamics is shown to generate an exponentially convergent dynamics. This property, together with assumptions on the inertia parameters of the rigid body, reveal instrumental to conclude on the exponential uniform convergence of the error dynamics. Importantly, the PE assumption is proven to be automatically satisfied in the particular case of free-rotation. In details, in Section IV, we establish that for almost all initial conditions, the PE assumption holds. This result stems from a detailed analysis of the various types of solutions to the free-rotation dynamics. Illustrative simulation results are given in Section V. Conclusions and perspectives are given in Section VI.

MINES ParisTech, PSL Research University, CAS, 60 bd Saint-Michel, 75272 Paris Cedex FRANCE. E-mail: lionel.magnis@mines-paristech.fr .

MINES ParisTech, PSL Research University, CAS, 60 bd Saint-Michel, 75272 Paris Cedex FRANCE. E-mail: nicolas.petit@mines-paristech.fr . Phone: +33140519330

II. NOTATIONS AND PROBLEM STATEMENT

A. Notations

Vectors in \mathbf{R}^3 are written with small letters x . $|x|$ is the Euclidean norm of x . $[x_\times]$ is the skew-symmetric cross-product matrix associated with x , i.e. $\forall y \in \mathbf{R}^3$, $[x_\times]y = x \times y$. Namely,

$$[x_\times] \triangleq \begin{pmatrix} 0 & -x_3 & x_2 \\ x_3 & 0 & -x_1 \\ -x_2 & x_1 & 0 \end{pmatrix}$$

where x_1, x_2, x_3 are the coordinates of x in the standard basis of \mathbf{R}^3 . If x is a unit vector, we have

$$[x_\times]^2 = xx^\top - I$$

Vectors in \mathbf{R}^6 are written with capital letters X . $|X|$ is the Euclidean norm of X . The induced norm on 6×6 matrices is denoted by $\|\cdot\|$. Namely,

$$\|M\| = \max_{|X|=1} |MX|$$

For convenience, we may write X under the form

$$X = \left(X_1^\top, X_2^\top \right)^\top$$

with $X_1, X_2 \in \mathbf{R}^3$. Note that

$$|X|^2 = |X_1|^2 + |X_2|^2$$

Frames considered in the following are orthonormal bases of \mathbf{R}^3 .

Rotation matrix. For any unit vector $u \in \mathbf{R}^3$ and any $\zeta \in \mathbf{R}$, $r_u(\zeta)$ designates the rotation matrix of axis u and angle ζ . Namely

$$r_u(\zeta) \triangleq \cos \zeta I + \sin \zeta [u_\times] + (1 - \cos \zeta) uu^\top$$

Circular functions \cos, \sin may, for brevity, be written c, s respectively.

B. Problem statement

Consider a rigid body rotating with respect to an inertial frame \mathcal{R}_i . Denote by R the rotation matrix from \mathcal{R}_i to a body frame \mathcal{R}_b attached to the rigid body and ω the corresponding angular velocity vector, expressed in \mathcal{R}_b . Assuming that the body rotates under the influence of an external torque τ (which, is null in the case of free-rotation), the variables R and ω are governed by the following differential equations

$$\dot{R} = R[\omega_\times] \quad (1)$$

$$\dot{\omega} = J^{-1} (J\omega \times \omega + \tau) \triangleq E(\omega) + J^{-1}\tau \quad (2)$$

where $J = \text{diag}(J_1, J_2, J_3)$ is the inertia matrix¹. Equation (2) is known as the set of Euler equations for a rotating rigid body [20]. The torque τ may result from control inputs or disturbances². We assume that J and τ are known.

Consider a reference unit vector \mathbf{a} expressed in \mathcal{R}_i . We assume that \mathbf{a} is constant, but it needs not be known. We consider that sensors arranged on the rigid body allow to measure the corresponding unit vector expressed in \mathcal{R}_b . Namely, the measurements are

$$a(t) \triangleq R(t)^\top \mathbf{a} \quad (3)$$

For implementation, the sensors could be e.g. accelerometers, magnetometers, or Sun sensors to name a few [21]. We now formulate some assumptions.

Assumption 1. ω is bounded: $|\omega(t)| \leq \omega_{\max}$ at all times

Assumption 2 (persistent excitation). *There exist constant parameters $T > 0$ and $0 < \mu < 1$ such that $a(\cdot)$ satisfies*

$$\frac{1}{T} \int_t^{t+T} [a(\tau)_\times]^\top [a(\tau)_\times] d\tau \geq \mu I, \quad \forall t \quad (4)$$

The problem we address in this paper is the following.

Problem 1. *Under Assumptions 1-2, find an estimate $\hat{\omega}$ of ω from the measurements a defined in (3).*

Remark 1 (on the persistent excitation). (4) is equivalent to

$$\frac{1}{T} \int_t^{t+T} \left(x^\top a(\tau) \right)^2 d\tau \leq 1 - \mu, \quad \forall t, \quad \forall |x| = 1 \quad (5)$$

which is only possible if $a(\cdot)$ varies uniformly on every interval $[t, t+T]$. Without the PE assumption, Problem 1 may not have a solution. For example, the initial conditions

$$a(t_0) = \begin{pmatrix} 1 \\ 0 \\ 0 \end{pmatrix}, \quad \omega(t_0) = \begin{pmatrix} w \\ 0 \\ 0 \end{pmatrix}$$

yield $a(t) = a(t_0)$ for all t , regardless of the value of w . Hence, the system is clearly not observable. Such a case is discarded by the PE assumption. Note that this assumption bears on the trajectory, hence on the initial condition $X(t_0)$ and on the torque τ only.

¹Without restriction, we consider that the axes of \mathcal{R}_b are aligned with the principal axes of inertia of the rigid body.

²In the case of a satellite e.g., the torque could be generated by inertia wheels, magnetorquers, gravity gradient, among other possibilities.

III. OBSERVER DEFINITION AND ANALYSIS OF CONVERGENCE

A. Observer definition

The time derivative of the measurement a is

$$\dot{a} = \dot{R}^\top \mathbf{a} = -[\omega_\times] R^\top \mathbf{a} = a \times \omega$$

To solve Problem 1, the main idea of the paper is to consider the reconstruction of the extended 6-dimensional state X by its estimate \hat{X}

$$X = \begin{pmatrix} a \\ \omega \end{pmatrix}, \quad \hat{X} = \begin{pmatrix} \hat{a} \\ \hat{\omega} \end{pmatrix}$$

The state is governed by

$$\dot{X} = \begin{pmatrix} a \times \omega \\ E(\omega) + J^{-1}\tau \end{pmatrix}$$

and the following observer is proposed

$$\dot{\hat{X}} = \begin{pmatrix} a \times \hat{\omega} - k(\hat{a} - a) \\ E(\hat{\omega}) + J^{-1}\tau + k^2 a \times (\hat{a} - a) \end{pmatrix} \quad (6)$$

where $k > 0$ is a constant (tuning) parameter. Denote

$$\tilde{X} \triangleq X - \hat{X} \triangleq \begin{pmatrix} \tilde{a} \\ \tilde{\omega} \end{pmatrix} \quad (7)$$

the error state. We have

$$\dot{\tilde{X}} = \begin{pmatrix} -kI & [a_\times] \\ k^2[a_\times] & 0 \end{pmatrix} \tilde{X} + \begin{pmatrix} 0 \\ E(\omega) - E(\hat{\omega}) \end{pmatrix} \quad (8)$$

B. Preliminary change of variables and properties

The study of the dynamics (8) employs a preliminary change of coordinates. Denote

$$Z \triangleq \begin{pmatrix} \tilde{a} \\ \frac{\tilde{\omega}}{k} \end{pmatrix} \quad (9)$$

yielding

$$\dot{Z} = kA(t)Z + \begin{pmatrix} 0 \\ \frac{E(\omega) - E(\hat{\omega})}{k} \end{pmatrix} \quad (10)$$

with

$$A(t) \triangleq \begin{pmatrix} -I & [a(t)_\times] \\ [a(t)_\times] & 0 \end{pmatrix} \quad (11)$$

which we will analyze as an ideal linear time-varying (LTV) system

$$\dot{Z} = kA(t)Z \quad (12)$$

disturbed by the input term

$$\xi \triangleq \begin{pmatrix} 0 \\ \frac{E(\omega) - E(\hat{\omega})}{k} \end{pmatrix} \quad (13)$$

We start by upper-bounding the disturbance (13).

Proposition 1 (Bound on the disturbance). *For any Z , ξ is bounded by*

$$|\xi| \leq d(\sqrt{2}\omega_{\max}|Z| + k|Z|^2) \quad (14)$$

where d is defined as

$$d \triangleq \max \left\{ \left| \frac{J_3 - J_2}{J_1} \right|, \left| \frac{J_1 - J_3}{J_2} \right|, \left| \frac{J_2 - J_1}{J_3} \right| \right\} \quad (15)$$

Proof. We have

$$|\xi| = \frac{1}{k} |E(\omega) - E(\hat{\omega})|$$

with, due to the quadratic nature of $E(\cdot)$,

$$\begin{aligned} E(\omega) - E(\hat{\omega}) &= J^{-1} (J\tilde{\omega} \times \omega + J\omega \times \tilde{\omega} - J\tilde{\omega} \times \tilde{\omega}) \\ &= \begin{pmatrix} \frac{J_2 - J_3}{J_1} (\omega_2 \tilde{\omega}_3 + \tilde{\omega}_2 \omega_3) \\ \frac{J_3 - J_1}{J_2} (\omega_3 \tilde{\omega}_1 + \tilde{\omega}_3 \omega_1) \\ \frac{J_1 - J_2}{J_3} (\omega_1 \tilde{\omega}_2 + \tilde{\omega}_1 \omega_2) \end{pmatrix} - \begin{pmatrix} \frac{J_2 - J_3}{J_1} \tilde{\omega}_2 \tilde{\omega}_3 \\ \frac{J_3 - J_1}{J_2} \tilde{\omega}_3 \tilde{\omega}_1 \\ \frac{J_1 - J_2}{J_3} \tilde{\omega}_1 \tilde{\omega}_2 \end{pmatrix} \\ &\triangleq \delta_1 - \delta_2 \end{aligned}$$

As a straightforward consequence

$$|\delta_2| \leq d|\tilde{\omega}|^2$$

Moreover, by Cauchy-Schwarz inequality

$$(\omega_2\tilde{\omega}_3 + \tilde{\omega}_2\omega_3)^2 \leq (\omega_2^2 + \omega_3^2)(\tilde{\omega}_2^2 + \tilde{\omega}_3^2) \leq (\omega_2^2 + \omega_3^2)|\tilde{\omega}|^2$$

Using similar inequalities for all the coordinates of δ_1 yields

$$|\delta_1|^2 \leq 2d^2|\omega|^2|\tilde{\omega}|^2 \leq 2d^2\omega_{\max}^2|\tilde{\omega}|^2$$

Hence,

$$\begin{aligned} |\xi| &\leq \frac{|\delta_1| + |\delta_2|}{k} \leq d\sqrt{2}\omega_{\max} \left| \frac{\tilde{\omega}}{k} \right| + kd \left| \frac{\tilde{\omega}}{k} \right|^2 \\ &\leq d(\sqrt{2}\omega_{\max}|Z| + k|Z|^2) \end{aligned}$$

□

Remark 2 (on the quantity d). As J_1, J_2, J_3 are the main moments of inertia of the rigid body, we have [20] (§32,9)

$$J_i \leq J_j + J_k$$

for all permutations i, j, k and hence $0 \leq d \leq 1$. Moreover, $d = 0$ if and only if $J_1 = J_2 = J_3$. d appears as a measurement of how far the rigid body is from an ideal symmetric body. For this reason, we call it discordance of the rigid body. Examples:

- For a homogeneous parallelepiped of size $l \times l \times L$, with $L \geq l$, we have

$$d = \frac{L^2 - l^2}{L^2 + l^2}$$

- For a homogeneous straight cylinder of radius r and height h we have

$$d = \frac{|h^2 - 3r^2|}{h^2 + 3r^2}$$

C. Analysis of the LTV dynamics $\dot{Z} = kA(t)Z$

The shape of $A(t)$ will appear familiar to the reader acquainted with adaptive control problems. Along the trajectories of (12) we have

$$\frac{d}{dt}|Z|^2 = -2k|Z_1|^2 = -Z^\top C^\top C Z$$

with

$$C \triangleq (\sqrt{2k}I \quad 0)$$

As will be seen in the proof of the following Theorem, the PE assumption will imply, in turn, that the pair $(kA(\cdot), C)$ is uniformly completely observable (UCO), which guarantees uniform exponential stability of the LTV system.

Theorem 1 (LTV system exponential stability). *There exists $0 < c < 1$ depending only on T, μ, k and ω_{\max} such that the solution of (12) satisfies for all integer $N \geq 0$*

$$|Z(t)|^2 \leq c^N |Z(t_0)|^2, \quad \forall t \in [t_0 + NT, t_0 + (N+1)T]$$

for any initial condition $t_0, Z(t_0)$.

Proof. Along the trajectories of (12) we have

$$\frac{d}{dt}|Z|^2 = -2k|Z_1|^2 \leq 0$$

which proves the result for $N = 0$. For all t

$$|Z(t+T)|^2 = |Z(t)|^2 - Z(t)^2 W(t, t+T) Z(t)$$

where

$$W(t, t+T) \triangleq \int_t^{t+T} \phi(\tau, t)^\top C^\top C \phi(\tau, t) d\tau$$

is the observability Gramian of the pair $(kA(\cdot), C)$ and ϕ is the transition matrix associated with (12). Computing W is no easy task. However, the output injection UCO equivalence result presented in [22] allows us to consider a much simpler system. Denote

$$K(t) \triangleq \frac{\sqrt{k}}{\sqrt{2}} \begin{pmatrix} I \\ -[a(t)_\times] \end{pmatrix}$$

and

$$\begin{aligned} M(t) &\triangleq kA(t) + K(t)C \\ &= \begin{pmatrix} 0 & k[a(t)_\times] \\ 0 & 0 \end{pmatrix} \end{aligned}$$

The observability Gramian \widetilde{W} of the pair $(M(\cdot), C)$ is easily computed as

$$\widetilde{W}(t, t+T) = 2k \int_t^{t+T} \begin{pmatrix} I & \mathcal{A}(\tau, t) \\ \mathcal{A}(\tau, t)^\top & \mathcal{A}(\tau, t)^\top \mathcal{A}(\tau, t) \end{pmatrix} d\tau$$

where

$$\mathcal{A}(\tau, t) \triangleq k \int_t^\tau [a(u)_\times] du$$

Such a Gramian is well known in optimal control and has been extensively studied e.g. in [23], Lemma 13.4. We have

- $\int_t^{t+T} k[a(\tau)_\times]^\top k[a(\tau)_\times] d\tau \geq Tk^2\mu I, \quad \forall t$
- $k[a(\cdot)_\times]$ is bounded by k
- $\frac{d}{dt}k[a(\cdot)_\times]$ is bounded by $k\omega_{\max}$

from which we deduce that there exists $0 < \beta_1 < 1$ depending on T, μ, k, ω_{\max} such that

$$\widetilde{W}(t, t+T) \geq \beta_1 I, \quad \forall t$$

There also exists $\beta_2 > 0$ depending on k, T such that $\widetilde{W}(t, t+T) \leq \beta_2 I$. From [22], Lemma 4.8.1 (output injection UCO equivalence), $W(t, t+T)$ is also lower-bounded. More precisely, we have

$$W(t, t+T) \geq \frac{\beta_1}{2(1 + \beta_2 T k)} I \triangleq (1-c)I$$

with $c < 1$. Assume the result is true for an integer $N \geq 0$. For any $t \in [t_0 + NT, t_0 + (N+1)T]$ we have

$$\begin{aligned} |Z(t+T)|^2 &= |Z(t)|^2 - Z(t)^\top W(t, t+T) Z(t) \\ &\leq c|Z(t)|^2 \leq c^{N+1}|Z(t_0)|^2 \end{aligned}$$

which yields $c > 0$ (consider a non-zero solution) and concludes the proof by induction. \square

D. Convergence of the observer

Consider the quantity

$$d^* \triangleq \frac{1-c}{2\sqrt{2}T\omega_{\max}} \quad (16)$$

where c is defined in Theorem 1. The following Theorem, which is the main result of the paper, shows that if $d < d^*$, the observer (6) provides a solution to Problem 1.

Theorem 2 (main result). *We suppose that Assumptions 1-2 are satisfied and that*

$$d < d^*$$

where d^* is defined in (16). The observer (6) defines an error dynamics (8) for which the equilibrium 0 is locally uniformly exponentially stable. The basin of attraction of this equilibrium contains the ellipsoid

$$\left\{ \tilde{X}(0), \quad |\tilde{a}(0)|^2 + \frac{|\tilde{\omega}(0)|^2}{k^2} < r^2 \right\} \quad (17)$$

with

$$r^2 \triangleq \frac{(1-c)^3}{8\sqrt{3}d^2T^3k^3} \left(1 - \frac{2\sqrt{2}dT\omega_{\max}}{1-c} \right)^2 \quad (18)$$

Proof. Consider the candidate Lyapunov function

$$V(t, Z) \triangleq Z^\top \left(\int_t^{+\infty} \phi(\tau, t)^\top \phi(\tau, t) d\tau \right) Z$$

where ϕ is the transition matrix of system (12). Let (t, Z) be fixed. One easily shows that $\|kA(t)\| \leq k\sqrt{3}$ for all t . Thus (see for example [24] Theorem 4.12)

$$V(t, Z) \geq \frac{1}{2k\sqrt{3}} |Z|^2 \triangleq c_1 |Z|^2 \triangleq W_1(Z)$$

Moreover, Theorem 1 implies that

$$\begin{aligned} V(t, Z) &= \sum_{N=0}^{+\infty} \int_{t+NT}^{t+(N+1)T} Z^\top \phi(\tau, t)^\top \phi(\tau, t) Z \\ &\leq T \sum_{N=0}^{+\infty} c^N |Z|^2 = \frac{T}{1-c} |Z|^2 \\ &\triangleq c_2 |Z|^2 \triangleq W_2(Z) \end{aligned}$$

This inequality, which holds for any value of Z , implies that the largest eigenvalue of the symmetric positive matrix

$$Q(t) \triangleq \int_t^{+\infty} \phi(\tau, t)^\top \phi(\tau, t) d\tau$$

is smaller than $\frac{T}{1-c}$.

By construction, V satisfies

$$\frac{\partial V}{\partial t}(t, Z) + \nabla V(t, Z)^\top kA(t)Z = -|Z|^2$$

where ∇ is the gradient with respect to Z . Hence, the derivative of V along the trajectories of (10) is

$$\frac{d}{dt}V(t, Z) = -|Z|^2 + \nabla V(t, Z)^\top \xi$$

Using

$$|\nabla V(t, Z)| = 2|Q(t)Z| \leq \frac{2T}{1-c}|Z|$$

together with inequality (14) and the Cauchy-Schwarz inequality yields

$$\left| \nabla V(t, Z)^\top \xi \right| \leq \frac{2dT}{1-c} \left(\sqrt{2\omega_{\max}}|Z|^2 + k|Z|^3 \right)$$

Hence

$$\begin{aligned} \frac{d}{dt}V(t, Z) &\leq -|Z|^2 \left(1 - \frac{2\sqrt{2}dT\omega_{\max}}{1-c} - \frac{2dT k}{1-c}|Z| \right) \\ &\triangleq -W_3(Z) \end{aligned}$$

By assumption $d < d^*$, which implies

$$1 - \frac{2\sqrt{2}dT\omega_{\max}}{1-c} > 0$$

We proceed as in [24] Theorem 4.9. If the initial condition of (10) satisfies

$$\begin{aligned} |Z(t_0)| &< r \\ \Leftrightarrow |Z(t_0)| &< \frac{1-c}{2dkT} \left(1 - \frac{2\sqrt{2}dT\omega_{\max}}{1-c} \right) \times \sqrt{\frac{c_1}{c_2}} \end{aligned}$$

then $W_3(Z(t_0)) > 0$ and, while $W_3(Z(t)) > 0$, $Z(\cdot)$ remains bounded by

$$|Z(t)|^2 \leq \frac{V(t)}{c_1} \leq \frac{V(t_0)}{c_1} \leq \frac{c_2}{c_1} |Z(t_0)|^2$$

which shows that

$$\begin{aligned} W_3(Z) &\geq \left(1 - \frac{2\sqrt{2}dT\omega_{\max}}{1-c} - \frac{2dkT}{1-c} \sqrt{\frac{c_2}{c_1}} |Z(t_0)| \right) |Z|^2 \\ &\triangleq c_3 |Z|^2 \end{aligned}$$

Consequently

$$|Z(t)|^2 \leq \frac{c_2}{c_1} e^{-\frac{c_3}{c_2}(t-t_0)} |Z(t_0)|^2$$

which shows that the equilibrium 0 of system (10) is locally uniformly exponentially stable. From (9), one directly deduces that the basin of attraction contains the ellipsoid (17). \square

Remark 3. *The limitations imposed on $\tilde{a}(0)$ in (17) are not truly restrictive because, as the actual value $a(0)$ is assumed known, the observer may be initialized with $\tilde{a}(0) = 0$. What matters is that the error on the unknown quantity $\omega(0)$ can be large in practice.*

IV. PE ASSUMPTION IN FREE-ROTATION

The PE Assumption 2 is the cornerstone of the proof of the main result. It is interesting to investigate whether it is often satisfied in practice (we have seen in Remark 1 that it might fail). In this section we consider a free-rotation dynamics, namely $\tau = 0$. We will prove that Assumption 2, or equivalently condition (5), is satisfied for almost all initial conditions.

The following important properties hold.

- $\omega^\top J\omega$ is constant over time (which implies that Assumption 1 is satisfied)
- The *moment of inertia* of the rigid body expressed in the inertial frame

$$\mathbf{m} \triangleq R(t)J\omega(t) \tag{19}$$

is constant over time.

- Thus, any trajectory $t \mapsto \omega(t)$ lies on the intersection of two ellipsoids

$$\omega^\top J\omega = \omega(t_0)^\top J\omega(t_0), \quad \omega^\top J^2\omega = \omega(t_0)^\top J^2\omega(t_0)$$

The analysis of the intersection of those ellipsoids is quite involved and has been extensively studied in e.g. [20]. It follows that there are four kinds of trajectories for the solutions ω of (2). We list them below, where $(\omega_1, \omega_2, \omega_3)$ are the coordinates of ω in the body frame.

Type 1 ω is constant, which is observed if and only if $\omega(t_0)$ is an eigenvector of J .

Type 2 $J_1 > J_2 > J_3$ *singular case*: $\omega_1(t)$ and $\omega_3(t)$ vanish, $\omega_2(t)$ tends to a constant when t goes to infinity. This situation is observed only for a zero-measure set of initial conditions $\omega(t_0)$.

Type 3 $J_1 > J_2 > J_3$ *regular case*: the trajectory is periodic and not contained in a plane. This situation is observed for almost all initial conditions $\omega(t_0)$.

Type 4 the trajectory is periodic and draws a non-zero diameter circle. This situation is observed if and only if two moments of inertia are equal and $\omega(t_0)$ is not an eigenvector of J .

Examples of such trajectories are given in Figures 1-2 for various initial conditions. For convenience of visualization, we chose solutions having the same angular momentum norm $|\mathbf{m}|$, so that they lie on the surface of the same ellipsoid.

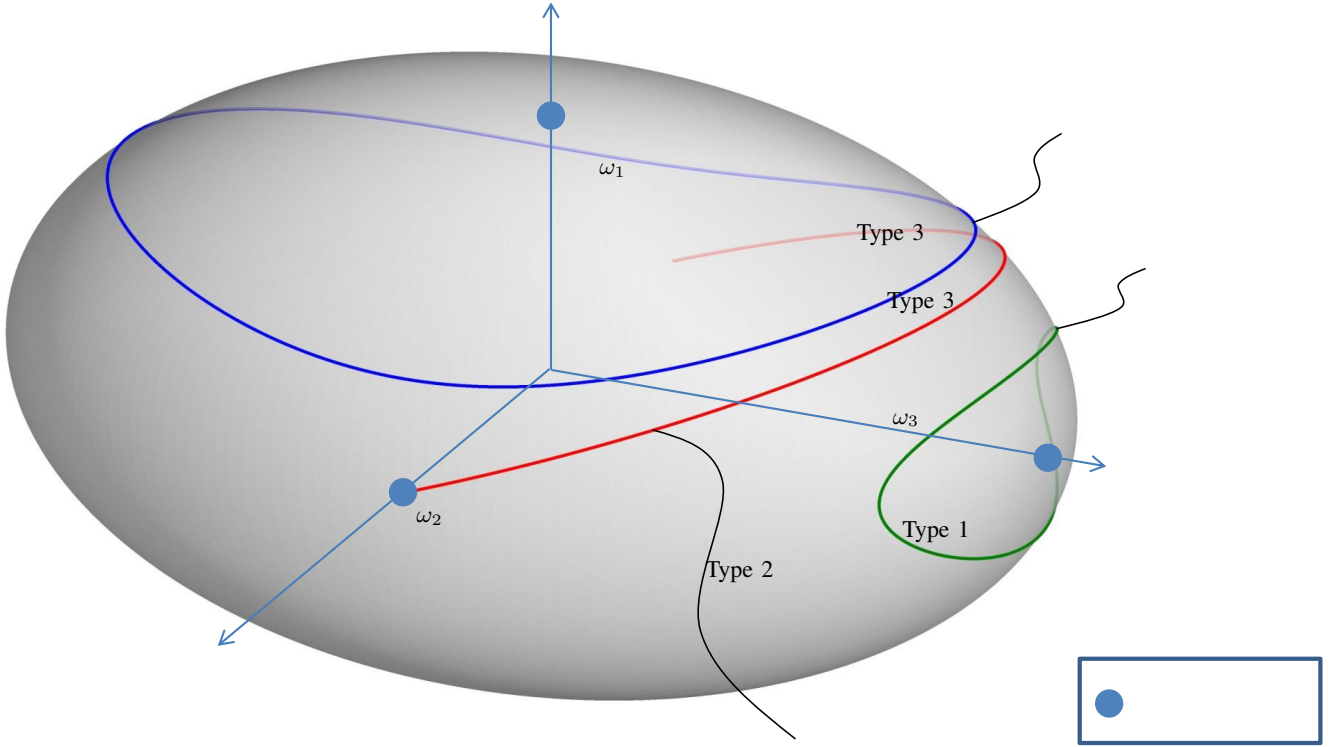


Fig. 1. Types 1,2 and 3 solutions having the same angular momentum norm $|\mathbf{m}|$.

A. Study of Type 1 and Type 2 solutions

The simplest case one can imagine is when $\omega(t_0)$ (or simply ω) is an eigenvector of J , namely for $i = 1, 2$ or 3

$$J\omega = J_i\omega$$

Denote

$$R_0 \triangleq R(t_0), \quad w \triangleq |\omega|, \quad u \triangleq \frac{1}{w}R_0\omega$$

Proposition 2. For all t , $R(t)$ can be written as

$$R(t) = r_u(w(t - t_0))R_0$$

where

$$r_u(w(t - t_0)) = w(t - t_0)I + s w(t - t_0)[u_\times] + (1 - c w(t - t_0))uu^\top$$

and where c, s stand for \cos, \sin respectively.

Proof. For convenience and without loss of generality, we take $t_0 = 0$ in the proof. $R(t)$ and $r_u(wt)R_0$ have the same value $R(t_0)$ for $t = t_0$. Moreover,

$$\begin{aligned} \frac{d}{dt}r_u(wt)R_0 &= w \left(-s wtI + c wt[u_\times] + s wt uu^\top \right) R_0 \\ &= (c wt[u_\times] + s wt[u_\times]^2) w R_0 \\ &= (c wtI + s wt[u_\times]) w[u_\times] R_0 \\ &= \left(c wtI + s wt[u_\times] + (1 - c wt)uu^\top \right) w[u_\times] R_0 \\ &= r_u(wt)w[u_\times] R_0 \\ &= r_u(wt)[R_0\omega_\times] R_0 = r_u(wt)R_0[\omega_\times] \end{aligned}$$

Thus both functions satisfy (1), which concludes the proof by Cauchy-Lipschitz uniqueness theorem. \square

It follows that for all t , $a(t)$ can be written as

$$\begin{aligned} a(t) &= R(t)^\top \mathbf{a} \\ &= c \, wt R_0^\top \mathbf{a} - s \, wt R_0^\top (u \times \mathbf{a}) + (1 - c \, wt) u^\top \mathbf{a} R_0^\top u \end{aligned} \quad (20)$$

For this reason, we call *planar rotation* the $R(\cdot)$ matrix generated by a Type 1 trajectory.

Remark 4. The direction u of the rotation can be simply computed from \mathbf{m} . We have

$$\mathbf{m} = R J \omega = J_i R \omega = w J_i R R_0^\top u = w J_i u$$

which implies that

$$u = \frac{\mathbf{m}}{|\mathbf{m}|}$$

The impact of the planar nature of the rotation on the PE assumption is as explained in the next two subsections.

1) *Type 1 solution with \mathbf{m} aligned with \mathbf{a} or $\omega = 0$:* Consider that \mathbf{a} is aligned with $\mathbf{m} = R(t_0) J \omega(t_0)$. In this case $u = \pm \mathbf{a}$ (see Remark 4). Thus, (20) yields $a(t) = R_0^\top \mathbf{a}$ constant over time. This also holds when $\omega(t_0) = 0$. For any T we have, for the unit vector $x = R_0^\top \mathbf{a}$

$$\frac{1}{T} \int_0^T (a(s)^\top x)^2 ds = 1$$

Thus, condition (5) is not satisfied.

2) *Type 1 solution with \mathbf{m} not aligned with \mathbf{a} :* Conversely, consider that \mathbf{a} is not aligned with \mathbf{m} . Define v, z such that (u, v, z) is a direct orthonormal basis of \mathbf{R}^3 . The decomposition of the unit vector \mathbf{a} in this basis is given as

$$\mathbf{a} = a_1 u + a_2 v + a_3 z, \quad a_1^2 + a_2^2 + a_3^2 = 1, \quad \text{with } a_1^2 < 1$$

We have

$$a(t) = R_0^\top (a_1 u + (a_2 c \, wt + a_3 s \, wt) v + (a_3 c \, wt - a_2 s \, wt) z)$$

For $T = \frac{2\pi}{w}$, any t and any unit vector

$$x = R_0^\top (x_1 u + x_2 v + x_3 z)$$

we have

$$\begin{aligned} &\frac{1}{T} \int_t^{t+T} (a(s)^\top x)^2 ds = \\ &\frac{1}{T} \int_t^{t+T} (a_1 x_1 + (a_2 c \, wt + a_3 s \, wt) x_2 + (a_3 c \, wt - a_2 s \, wt) x_3)^2 ds \\ &= a_1^2 x_1^2 + \frac{a_2^2 + a_3^2}{2} (x_2^2 + x_3^2) \leq (1 - \mu) \end{aligned}$$

with

$$\mu \triangleq \min \left(1 - a_1^2, \frac{1 + a_1^2}{2} \right) \in (0, 1)$$

Thus, condition (5) is satisfied.

3) *Type 2 solutions:* As shown in [20], the Type 2 solutions are characterized by $J_1 > J_2 > J_3$ and

$$|\omega_1(t_0)| = \sqrt{\frac{J_3(J_2 - J_3)}{J_1(J_1 - J_2)}} |\omega_3(t_0)| \neq 0$$

which defines a zero-measure set. For this reason, they are called *singular* solutions. In this case, $\omega(t)$ converges to a limit $\omega_\infty = (0, \pm w, 0)$, which is an eigenvector of J , when t goes to infinity. The rotation $R(t)$ is thus asymptotically arbitrarily close to a planar rotation around $\mathbf{m} = R(t_0) J \omega(t_0)$. The arguments already employed for the Type 1 solutions show that condition (5) is satisfied unless $R(t_0) J \omega(0)$ and \mathbf{a} are aligned.

B. Study of Type 3 and Type 4 solutions

In this section we will show that the Type 3 and Type 4 solutions satisfy the PE assumption. Both proofs relies on the following technical result.

Proposition 3 (preliminary result). *If condition (4) is not satisfied, then for all $T > 0$ and all $\varepsilon > 0$ small enough, there exists t such that for all $y \in \mathbf{R}^3$, and all $s \in [t, t + T]$,*

- $R(s)y$ remains between two planes orthogonal to \mathbf{a} and distant by $\varepsilon|y|$
- $R(s)^\top y$ remains between two parallel planes distant by $\varepsilon|y|$.

Proof. Consider $T > 0$ and μ such that

$$0 < \mu < \min \left(\frac{1}{4T\omega_{\max}}, \frac{T\omega_{\max}}{4} \right) < 1 \quad (21)$$

Assume that (5) is not satisfied. There exists t, x such that $|x| = 1$ and

$$\frac{1}{T} \int_t^{t+T} \left(a(s)^\top x \right)^2 ds \geq 1 - \mu \quad (22)$$

As will appear, one can use the bounded variations of $a(\cdot)$ due to its governing dynamics to establish a lower bound on the integrand. Denote

$$h(s) \triangleq \left(a(s)^\top x \right)^2, \quad \forall s$$

We will now show by contradiction that

$$h(s) \geq 1 - 2\sqrt{T\omega_{\max}\mu}, \quad \forall s \in [t, t+T]$$

Assume that there exists s_0 such that

$$h(s_0) < 1 - 2\sqrt{T\omega_{\max}\mu}$$

We have, for all s ,

$$\begin{aligned} |\dot{h}(s)| &= \left| 2\dot{a}(s)^\top x a(s)^\top x \right| \\ &= \left| 2(a(s) \times \omega)^\top x a(s)^\top x \right| \leq 2\omega_{\max} \end{aligned}$$

Assume $s_0 \leq t + \frac{T}{2}$ and denote

$$s_1 \triangleq s_0 + \sqrt{\frac{T\mu}{\omega_{\max}}} \leq t + T$$

We have, for any $s \in [s_0, s_1] \subset [t, t+T]$

$$\begin{aligned} h(s) &\leq h(s_0) + 2\omega_{\max}(s - s_0) \\ &< 1 - 2\sqrt{T\omega_{\max}\mu} + 2\omega_{\max}(s - s_0) \end{aligned}$$

Hence

$$\begin{aligned} \frac{1}{T} \int_t^{t+T} \left(a(s)^\top x \right)^2 ds &< 1 - \frac{1}{T} \sqrt{\frac{T\mu}{\omega_{\max}}} \\ &\quad + \frac{1}{T} \int_{s_0}^{s_1} \left(1 - 2\sqrt{T\omega_{\max}\mu} + 2\omega_{\max}(s - s_0) \right) ds \\ &= 1 - 2\mu + \mu = 1 - \mu \end{aligned}$$

which contradicts (22). The case $s_0 > t + \frac{T}{2}$ is analog with $s \in [s_0 - \sqrt{\frac{T\mu}{\omega_{\max}}}, s_0] \subset [t, t+T]$. Finally, we have, for all s

$$0 < 1 - 2\sqrt{T\omega_{\max}\mu} \leq \left(a(s)^\top x \right)^2 \leq 1$$

which shows that the continuous function $s \mapsto a(s)^\top x$ is of constant sign, strictly positive without loss of generality. Thus, we have

$$0 < 1 - 2\sqrt{T\omega_{\max}\mu} \leq a(s)^\top x \leq 1$$

and in turn

$$|a(s) - x|^2 = 2 - 2a(s)^\top x \leq 4\sqrt{T\omega_{\max}\mu} \triangleq \gamma\sqrt{\mu} \quad (23)$$

Denote by R_1 a rotation matrix so that

$$\mathbf{a} = R_1 x$$

and, for all $s, u(s), \xi(s)$ such that

$$R(s) \triangleq r_{u(s)}(\xi(s))R_1$$

Note that $R(s)x = r_{u(s)}(\xi(s))\mathbf{a}$. The next Lemma formulates that the rotation $R(s)$ is uniformly close to $r_{\mathbf{a}}(\xi(s))R_1$.

Lemma 1. *We have, for all $s \in [t, t+T]$ and all $y \in \mathbf{R}^3$*

$$|R(s)y - r_{\mathbf{a}}(\xi(s))R_1 y|^2 \leq 30\gamma\sqrt{\mu}|y|^2 \quad (24)$$

where γ is defined by (23).

Proof. Let $s \in [t, t+T]$. For clarity we may omit the s dependency of u and ξ . Denote

$$\begin{aligned} \Delta &\triangleq R(s) - r_{\mathbf{a}}(\xi)R_1 \\ &= \left(\sin \xi ([u_\times] - [\mathbf{a}_\times]) + (1 - \cos \xi) (uu^\top - \mathbf{a}\mathbf{a}^\top) \right) R_1 \end{aligned}$$

If $\mathbf{a} = u(s)$, $\|\Delta\| = 0 \leq 30\gamma\sqrt{\mu}$. Otherwise, for $A = x$ we have, from (23)

$$\begin{aligned} |\Delta A|^2 &= |R(s)x - r_{\mathbf{a}}(\xi)R_1x|^2 = |R(s)x - \mathbf{a}|^2 \\ &= \left| x - R^\top(s)\mathbf{a} \right|^2 = |x - a(s)|^2 \leq \gamma\sqrt{\mu} \end{aligned}$$

Denote v, z so that (u, v, z) is an orthonormal basis of \mathbf{R}^3 and write

$$\mathbf{a} = a_1u + a_2v + a_3z, \quad a_1^2 + a_2^2 + a_3^2 = 1$$

We have

$$\begin{aligned} \gamma\sqrt{\mu} &\geq |R(s)x - \mathbf{a}|^2 = |(r_u(\xi) - I)\mathbf{a}| \\ &= |(a_2(c\xi - 1) - a_3s\xi)v + (a_2s\xi + a_3(c\xi - 1))z|^2 \\ &= 4(a_2^2 + a_3^2)\sin^2\frac{\xi}{2} \end{aligned}$$

Now, denote $B = R_1^\top \frac{u \times \mathbf{a}}{|u \times \mathbf{a}|}$. We have

$$B^\top A = \frac{(u \times \mathbf{a})^\top R_1x}{|u \times \mathbf{a}|} = \frac{(u \times \mathbf{a})^\top \mathbf{a}}{|u \times \mathbf{a}|} = 0$$

so that A and B are orthonormal. We have

$$\begin{aligned} |\Delta B|^2 &= \frac{\sin^2\frac{\xi}{2}}{a_2^2 + a_3^2} |u \times (u \times \mathbf{a}) - \mathbf{a} \times (u \times \mathbf{a})|^2 \\ &= \frac{\sin^2\frac{\xi}{2}}{a_2^2 + a_3^2} (1 - \mathbf{a}^\top u)^2 |u + \mathbf{a}|^2 \\ &= \frac{\sin^2\frac{\xi}{2}}{a_2^2 + a_3^2} 4(1 - a_1^2)^2 \\ &\leq 16(a_2^2 + a_3^2)\sin^2\frac{\xi}{2} \leq 4\gamma\sqrt{\mu} \end{aligned}$$

For $C = A \times B$ we have

$$\begin{aligned} |\Delta C|^2 &= |R(s)(A \times B) - r_{\mathbf{a}}(\xi)R_1(A \times B)|^2 \\ &= |R(s)A \times R(s)B - r_{\mathbf{a}}(\xi)R_1A \times r_{\mathbf{a}}(\xi)r_1B|^2 \\ &= |R(s)A \times \Delta B + \Delta A \times r_{\mathbf{a}}(\xi)R_1B|^2 \\ &\leq 2(\gamma\sqrt{\mu} + 4\gamma\sqrt{\mu}) = 10\gamma\sqrt{\mu} \end{aligned}$$

and the vectors A, B, C are orthonormal. Finally, for any vector

$$y = y_1A + y_2B + y_3C, \quad y_1^2 + y_2^2 + y_3^2 = |y|^2$$

we have

$$\begin{aligned} |\Delta y|^2 &= |y_1\Delta A + y_2\Delta B + y_3\Delta C|^2 \\ &\leq 3(y_1^2|\Delta A|^2 + y_2^2|\Delta B|^2 + y_3^2|\Delta C|^2) \\ &\leq 3(y_1^2 + y_2^2 + y_3^2)10\gamma\sqrt{\mu} = 30\gamma\sqrt{\mu}|y|^2 \end{aligned}$$

which concludes the proof of Lemma 1. \square

Denote by $\varepsilon = 2\sqrt{30\gamma\sqrt{\mu}}$ and consider any y in \mathbf{R}^3 and any s in $[t, t + T]$. On the one hand, $r_{\mathbf{a}}(\xi(s))R_1y$ lies on a circle orthogonal to \mathbf{a} . On the other hand,

$$|R(s)y - r_{\mathbf{a}}(\xi(s))R_1y| \leq \frac{\varepsilon}{2}|y|$$

This yields the first item of Proposition 3 as $\mu > 0$ is arbitrary small. Rewriting the result of Lemma 1 as

$$\left| R_1^\top r_{\mathbf{a}}(-\xi(s))y - R(s)^\top y \right|^2 \leq 30\gamma\sqrt{\mu}|y|^2$$

for any $s \in [t, t + T]$ and any y yields the second item and concludes the proof. \square

1) *Type 3 solutions*: These solutions are characterized by $J_1 > J_2 > J_3$ and

$$|\omega_1(t_0)| \neq \sqrt{\frac{J_3(J_2 - J_3)}{J_1(J_1 - J_2)}} |\omega_3(t_0)|$$

In this case the trajectory of $\omega(\cdot)$ is closed and thus periodic of a certain period $T_0 > 0$, and not contained in a plane. Assume that condition (5) is not satisfied. We apply the second item of Proposition 3 with $T = T_0$. For any ε small enough, there exists t such that for all $s \in [t, t + T_0]$

$$J\omega(s) = R^\top(s)\mathbf{m}$$

remains between two parallel planes and distant by $\varepsilon|\mathbf{m}|$. As $\omega(\cdot)$ is T_0 -periodic, this is true for all $s \in \mathbf{R}$. When ε goes to 0, we conclude that the trajectory of $\omega(\cdot)$ remains in a plane, which is a contradiction. Thus, condition (5) is satisfied, unconditionally on $R(t_0)$.

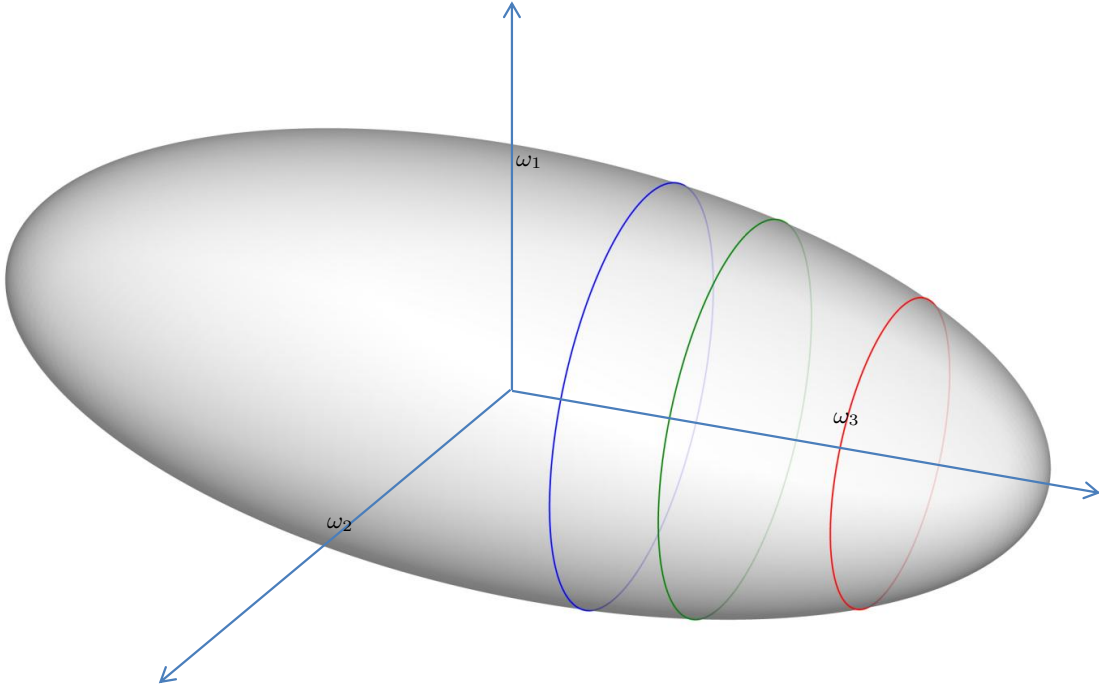


Fig. 2. Type 4 trajectories in the case $J_1 = J_2 > J_3$ having the same angular momentum norm $|\mathbf{m}|$.

2) *Type 4 solutions*: We now consider the case where $\omega(t_0)$ is not an eigenvector of J and two moments of inertia are equal. In this case the trajectory $t \mapsto \omega(t)$ is a circle, as represented in Figure 2. Since it is contained in a plane, we can not apply directly the same technique as for Type 3 solutions. Without loss of generality, we study the case $J_1 = J_2 > J_3$ (the case $J_1 > J_2 = J_3$ is analog). We thus consider a trajectory ω such that $\omega(0)$ satisfies

$$(\omega_1(t_0), \omega_2(t_0)) \neq (0, 0), \quad \omega_3(t_0) \neq 0$$

Following the extensive analysis exposed in [20], we conveniently chose the inertial frame (e_1, e_2, e_3) so that e_3 is aligned with \mathbf{m} , namely

$$e_3 = \frac{\mathbf{m}}{|\mathbf{m}|}$$

For this choice of e_3 and in the case where $J_1 = J_2$, equations (1)-(2) simplify considerably and one can show that the rotation matrix satisfies for all t

$$R(t) = p \begin{pmatrix} (\dots) & (\dots) & c \xi_1(t - t_1) \\ (\dots) & (\dots) & s \xi_1(t - t_1) \\ c \xi_2(t - t_2) & s \xi_2(t - t_2) & \frac{\sqrt{1-p^2}}{p} \end{pmatrix} \quad (25)$$

where (\dots) designates terms that are irrelevant in the following analysis, t_1, t_2 are constant and

$$\begin{aligned} p &\triangleq \sqrt{\frac{J_1^2 \omega_1(t_0)^2 + J_1^2 \omega_2(t_0)^2}{J_1^2 \omega_1(t_0)^2 + J_2^2 \omega_2(t_0)^2 + J_3^2 \omega_3(t_0)^2}} \in (0, 1) \\ \xi_1 &\triangleq \sqrt{\omega_1(t_0)^2 + \omega_2(t_0)^2 + \frac{J_3^2}{J_1^2} \omega_3(t_0)^2} > 0 \\ \xi_2 &\triangleq \left(\frac{J_3}{J_1} - 1 \right) \omega_3(t_0) \neq 0 \end{aligned}$$

We now show that condition (5) is satisfied by contradiction. Assuming that it is not, one can apply the first item of Proposition 3 with

$$T = \max \left(\frac{2\pi}{\xi_1}, \frac{2\pi}{|\xi_2|} \right)$$

For ε small enough, there exists t such that for all $s \in [t, t + T]$ $R(s)e_3$ remains between two planes orthogonal to \mathbf{a} and distant by ε . Moreover, expression (25) yields for all s

$$R(s)e_3 = \begin{pmatrix} p \cos \xi_1(s - t_1) \\ p \sin \xi_1(s - t_1) \\ \sqrt{1-p^2} \end{pmatrix}$$

Simple geometric considerations show that

$$\sqrt{1 - (\mathbf{a}^\top e_3)^2} \leq \frac{\varepsilon}{2p}$$

which yields $\mathbf{a} = \pm e_3$ when ε goes to 0. Hence for ε small enough, and all $s \in [t, t + T]$

$$R(s)e_1 = \begin{pmatrix} (\dots) \\ (\dots) \\ p \cos \xi_2(s - t_2) \end{pmatrix}$$

remains between two planes orthogonal to $\mathbf{a} = \pm e_3$. Taking $\varepsilon < 2p$ yields a contradiction. The trajectories $R(t)e_1$ and $R(t)e_3$ are represented in Figure 3 for better visual understanding of the proof.

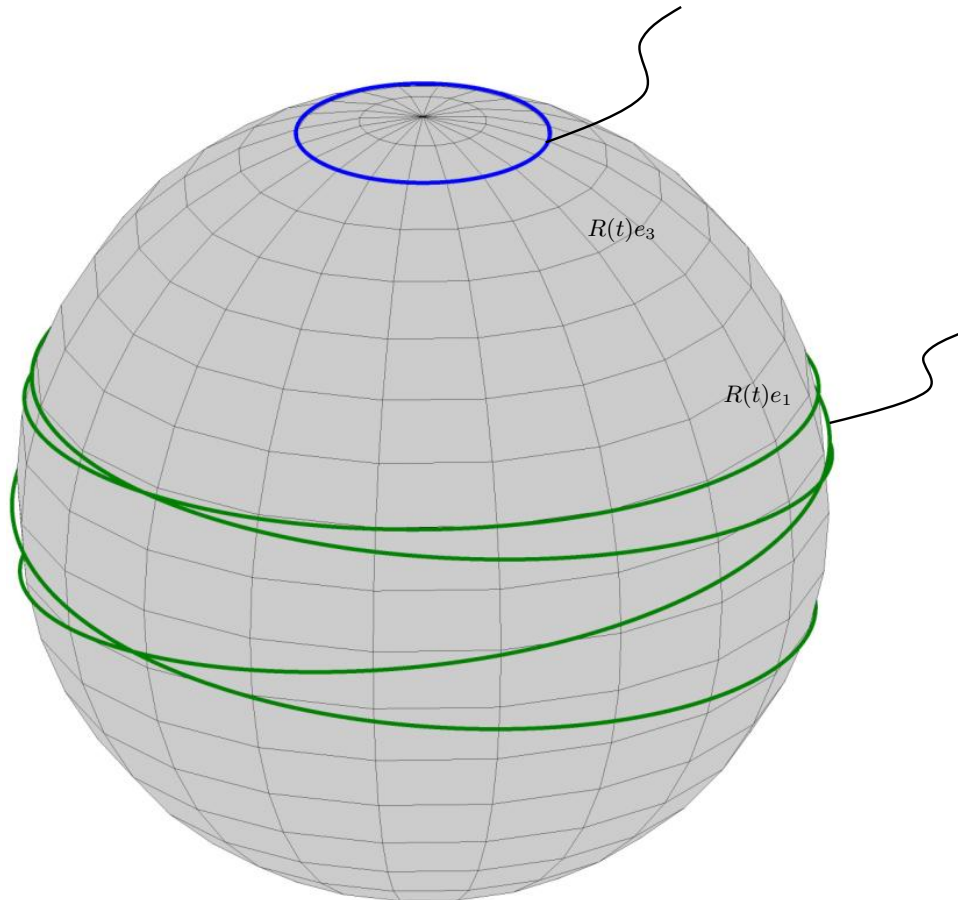


Fig. 3. $R(t)e_3$ and $R(t)e_1$ evolving on the unit sphere.

C. Conclusion

In this section we have shown the following result.

Theorem 3. Consider the vector

$$\mathbf{a}(t) = R(t)^\top \mathbf{a}$$

where $R(t)$ is a rotation matrix defined as the solution of the free-rotation dynamics (1)-(2) with $\tau = 0$. Assumption 2 is satisfied for almost all initial conditions $(R(t_0), \omega(t_0))$. It fails only in the cases listed below

- (i) $\omega(t_0)$ is an eigenvector of J and $R(t_0)J\omega(t_0)$ is aligned with \mathbf{a} , or
- (ii) the eigenvalues of J are of the form $J_1 > J_2 > J_3$, the coordinates of $\omega(t_0)$ in the trihedron of orthonormal eigendirections of J satisfy

$$|\omega_1(t_0)| = \sqrt{\frac{J_3(J_2 - J_3)}{J_1(J_1 - J_2)}} |\omega_3(t_0)| \quad (26)$$

and $R(t_0)J\omega(t_0)$ is aligned with \mathbf{a} .

It follows that, except for the initial conditions listed in items (i), (ii), the conclusion of Theorem 2 holds without requiring Assumption 2, which is automatically satisfied. Therefore, in almost all cases, observer (6) asymptotically reconstructs the desired angular velocity ω .

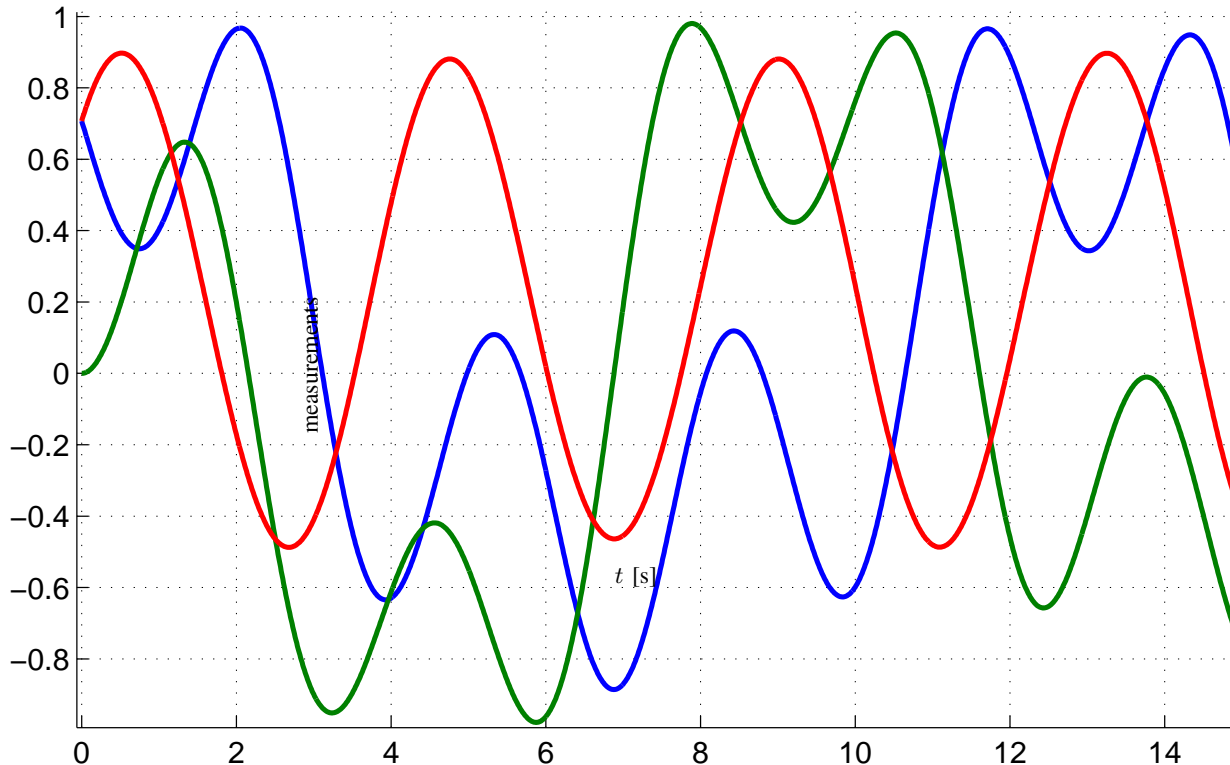


Fig. 4. Typical measurements in the ideal noise-free case.

V. SIMULATION RESULTS

In this section we illustrate the convergence of the observer and sketch the sensitivity with respect to the tuning gain k .

Simulations were run for a model of a CubeSat [25]. The rotating rigid body under consideration is a rectangular parallelepiped of dimensions about 20 cm \times 10 cm \times 10 cm and mass 2 kg assumed to be slightly non-homogeneously distributed. The resulting moments of inertia are

$$J_1 = 87 \text{ kg.cm}^2, \quad J_2 = 83 \text{ kg.cm}^2, \quad J_3 = 37 \text{ kg.cm}^2$$

No torque is applied on this system, which is thus in free-rotation. Referring to Section IV, we will consider Type 1 and Type 3 trajectories.

In this simulation the reference unit vector is the normalized magnetic field \mathbf{a} . The satellite is equipped with 3 magnetometers able to measure the normalized magnetic field y_a in a magnetometer frame \mathcal{R}_m .

It shall be noted that, in practical applications, the sensor frame \mathcal{R}_m can differ from the body frame \mathcal{R}_b (defined along the principal axes of inertia) through a constant rotation $R_{m,b}$. With these notations, we have

$$\mathbf{a} = R_{m,b}^\top y_a$$

which is a simple change of coordinates of the measurements.

For sake of accuracy in the implementation, reference dynamics and state observer (6) were simulated using Runge-Kutta 4 method with sample period 0.01s. The generated trajectories correspond to $\omega_{\max} \simeq 100$ [rad/s].

A. Noise-free simulations

To emphasize the role of the tuning gain k , we first assume that the sensors are perfect i.e. without noise. Typical measurements for a general Type 3 trajectory are represented in Figure 4. As J_1 and J_2 are almost equal, the third coordinate is almost (but not exactly) periodic. Figure 5 shows the convergence of the observer for various values of k . Interestingly, large values of k produce undesirable effects. This is a structural difference with the two reference vectors based observer previously introduced by the authors [19]. The reason is that the convergence is guaranteed by a PE argument and not by a uniformly negative bound on eigenvalues.

In Figure 6 we represented the observer error for a case where the PE assumption is not satisfied, namely for a constant ω with \mathbf{m} and $\mathbf{a} = (1 \ 0 \ 0)^\top$ aligned. This is a singular case, as discussed earlier. Interestingly, the coordinates $\tilde{\omega}_2$ and $\tilde{\omega}_3$ converge to zero, while $\tilde{\omega}_1$ converges to a constant value. This can easily be proved by using LaSalle's invariance principle. Indeed, in this case, ω and \mathbf{a} are constant and the error system (10) is actually LTI.

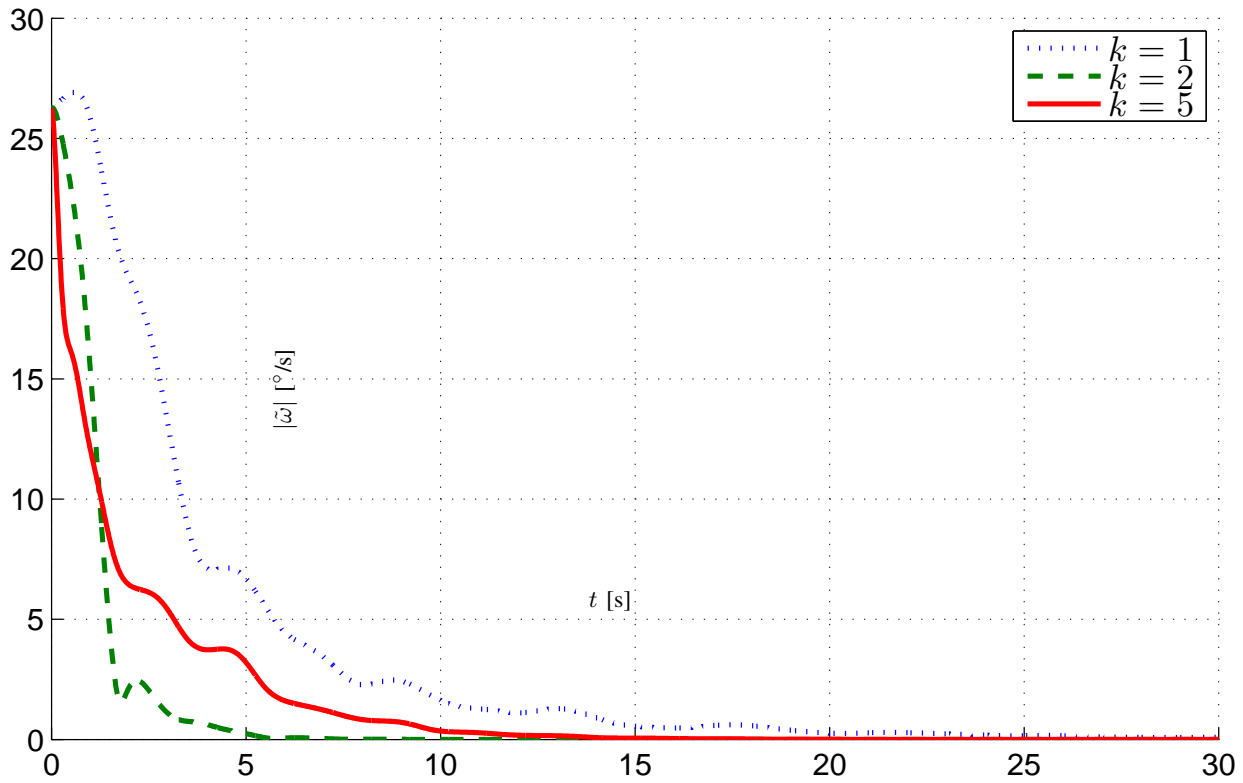


Fig. 5. Convergence of the observer for increasing values of k .

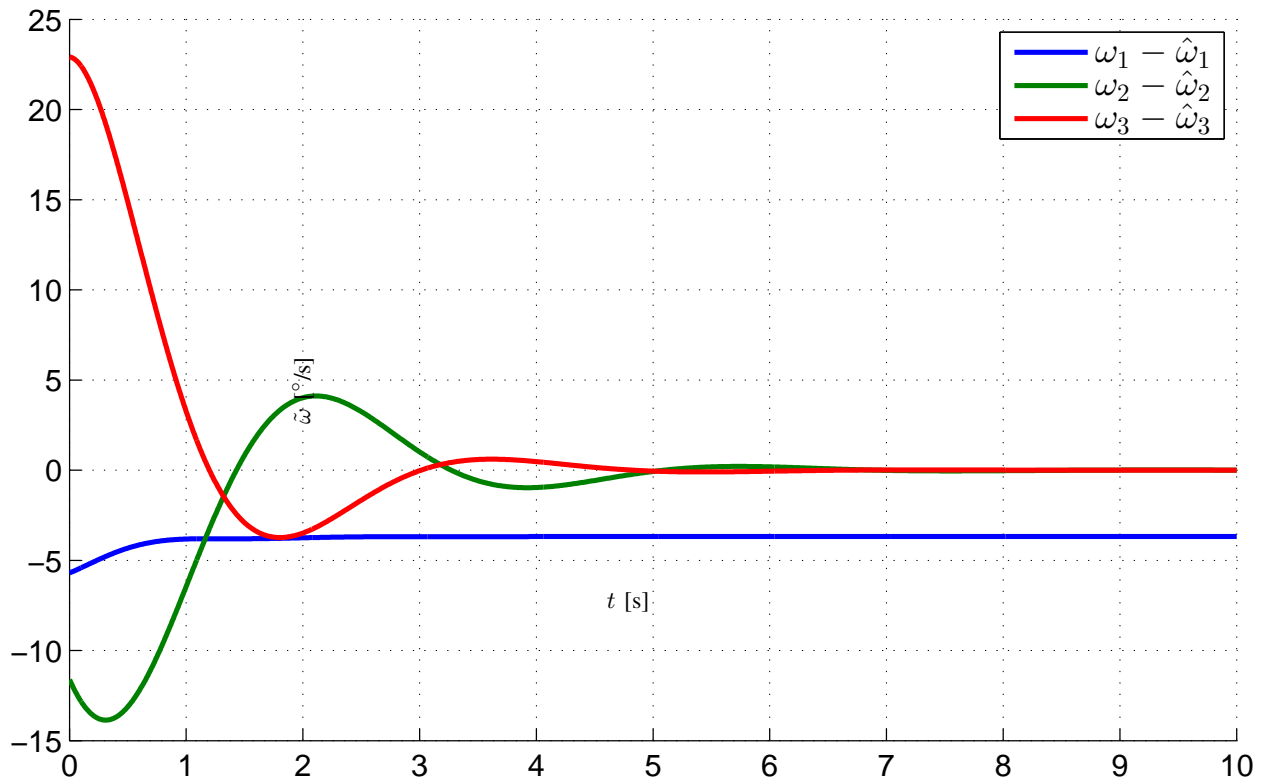


Fig. 6. Without the PE assumption asymptotic convergence of the observer is lost, a bias remains.

B. Measurement noise

We now study the impact of measurement noise on the observer performance. The simulation parameters remain the same but we add Gaussian measurement noise with standard deviation $\sigma = 0.03$ [Hz $^{-\frac{1}{2}}$]. Typical measurements are represented in Figure 7. The observer

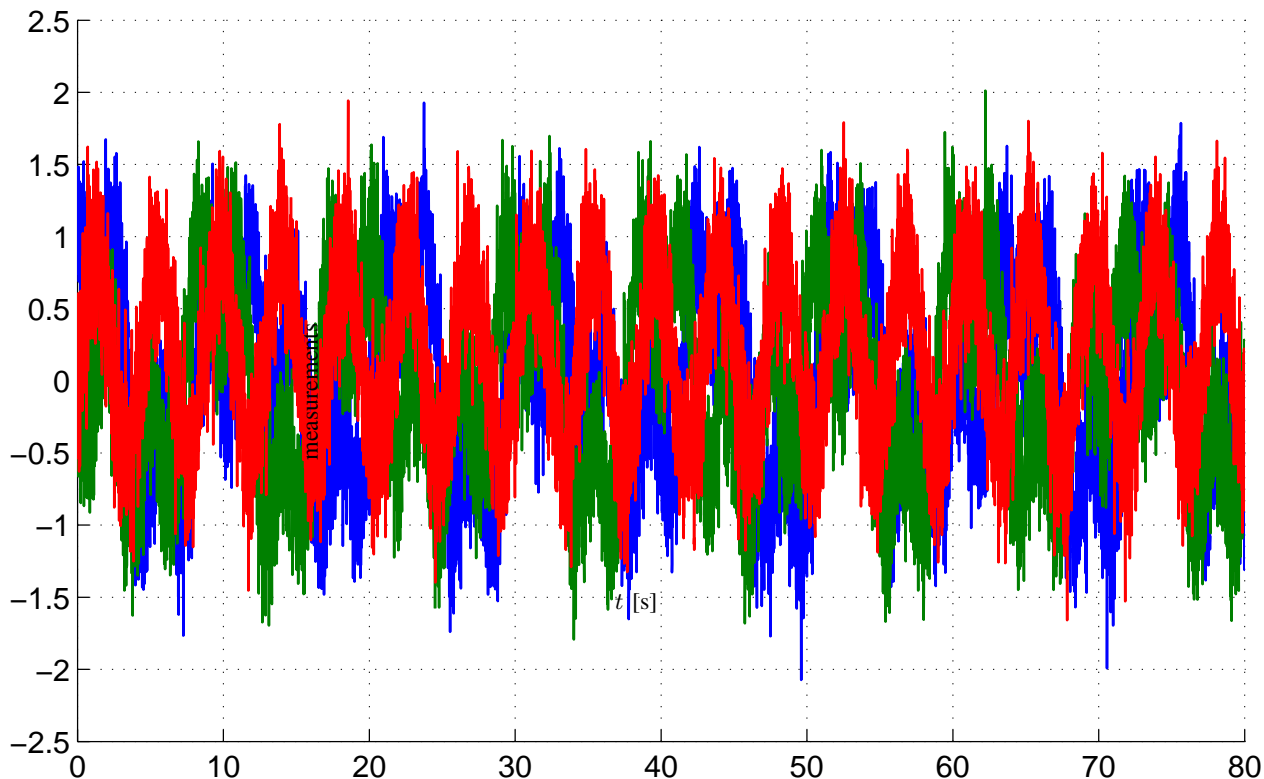


Fig. 7. Vector measurements with additive Gaussian noise.

yields a residual error, about 5% in Figure 8 for $k = 1$. Note that the measurement noise is filtered, thanks to a relatively low value of the gain k . For large values of k , the observer does not converge anymore (not represented).

VI. CONCLUSIONS AND PERSPECTIVES

A new method to estimate the angular velocity of a rigid body has been proposed in this article. The method uses onboard measurements of a single constant vector. The estimation algorithm is a nonlinear observer which is very simple to implement and induces a very limited computational burden. Moreover, it does not rely on the knowledge of the inertial coordinates of the reference vector, so that no reference model or look-up table are necessary. At this stage, an interesting (but still preliminary) conclusion is that, in the cases considered here, rate gyros could be replaced with an estimation software employing cheap, rugged and resilient sensors. In fact, any type of sensors producing a 3-dimensional vector of measurements such as e.g., Sun sensors, magnetometers, could constitute one such alternative. Assessing the feasibility of this approach requires further investigations including experiments.

More generally, this observer should be considered as a first element of a class of estimation methods which can be developed to address several cases of practical interest. In particular, the introduction of noise in the measurement and uncertainty on the input torque (assumed here to be known) will require extensions such as optimal filtering to treat more general cases. White or colored noises will be good candidates to model these elements. Also, slow variations of the reference vector should deserve particular care, because such drifts naturally appear in some cases.

On the other hand, one can also consider that this method can be useful for other estimation tasks. Among the possibilities are the estimation of the inertia J matrix which we believe is possible from the measurements considered here. This could be of interest for the recently considered task of space debris removal [26]. Finally, recent attitude estimation techniques have favored the use of vector measurements *together* with rate gyros measurements as inputs. Among these approaches, one can find *i*) Extended Kalman Filters (EKF)-like algorithms e.g. [27], [28], *ii*) nonlinear observers [29], [30], [31], [32], [33], [34]. This contribution suggests that, here also, the rate gyros could be replaced with more in-depth analysis of the vector measurements.

REFERENCES

- [1] S. Salcudean. A globally convergent angular velocity observer for rigid body motion. *IEEE Transactions on Automatic Control*, 36(12):1493–1497, 1991.
- [2] J. D. Bošković, S.-M. Li, and R. K. Mehra. A globally stable scheme for spacecraft control in the presence of sensor bias. *Proceedings of the IEEE Aerospace Conference*, pages 505–511, 2000.
- [3] E. Silani and M. Lovera. Magnetic spacecraft attitude control: a survey and some new results. *Control Engineering Practice*, 13:357–371, 2003.
- [4] M. Lovera and A. Astolfi. Global magnetic attitude control of inertially pointing spacecraft. *Journal of Guidance, Control, and Dynamics*, 28(5):1065–1072, 2005.
- [5] D. H. Titterton and J. L. Weston. *Strapdown Inertial Navigation Technology*. The American Institute of Aeronautics and Astronautics, 2nd edition, 2004.

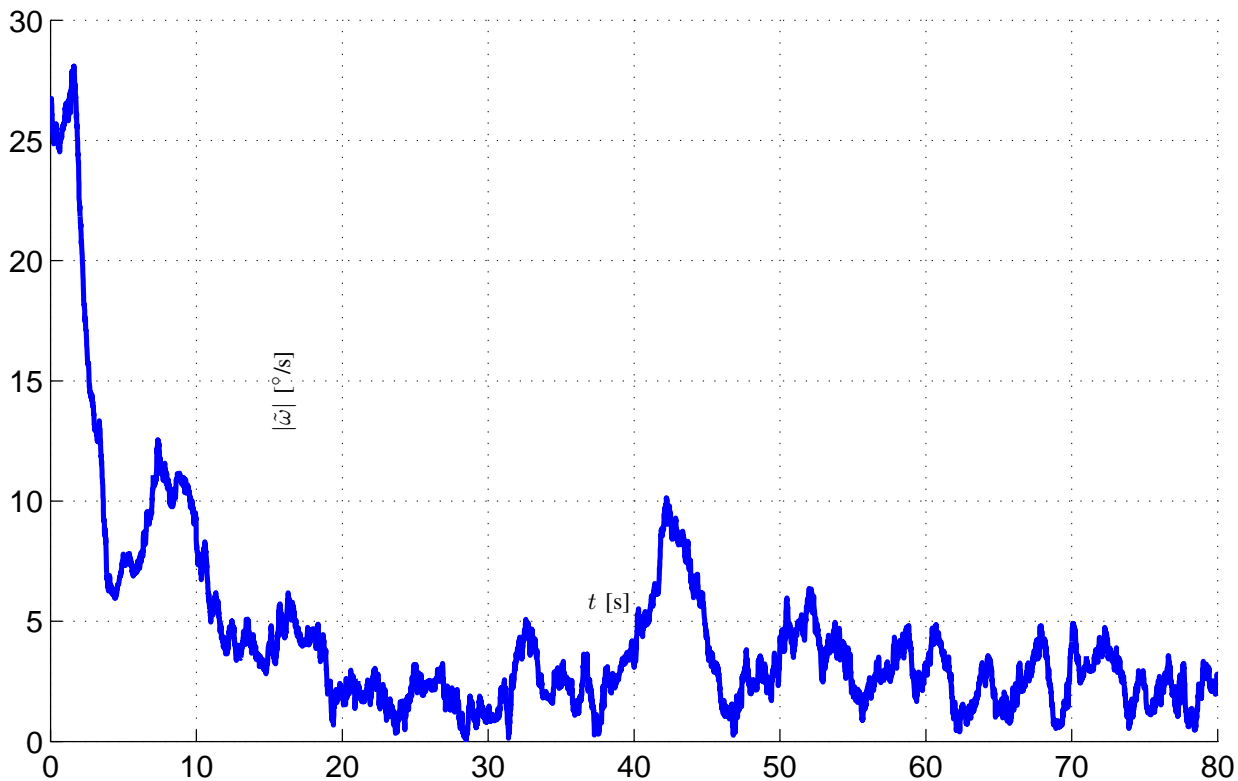


Fig. 8. Observer performance under noisy measurements for $k = 1$

- [6] I. Y. Bar-Itzhack. Classification of algorithms for angular velocity estimation. *Journal of Guidance, Control, and Dynamics*, 24(2):214–218, 2001.
- [7] Y. Oshman and F. Dellus. Spacecraft angular velocity estimation using sequential observations of a single directional vector. *Journal of Spacecraft and Rockets*, 40(2):237–247, 2003.
- [8] M. D. Lallo. Experience with the Hubble Space Telescope: 20 years of an archetype. *Optical Engineering*, 51(1), 2012.
- [9] D. C. Tsai, F. L. Markley, and T. P. Watson. SAMPEX spin stabilized mode. *Proceedings of the 10th International Conference on Space Operations*, 2008.
- [10] J. L. Crassidis, F. L. Markley, and Y. Cheng. Survey of nonlinear attitude estimation methods. *Journal of Guidance, Control, and Dynamics*, 30(1):12–28, 2007.
- [11] G. Wahba. Problem 65-1: a least squares estimate of spacecraft attitude. In *SIAM Review*, volume 7, page 409. 1965.
- [12] M. D. Shuster. Approximate algorithms for fast optimal attitude computation. *Proceedings of the AIAA Guidance and Control Conference*, pages 88–95, 1978.
- [13] M. D. Shuster. Kalman filtering of spacecraft attitude and the QUEST model. *The Journal of the Astronautical Sciences*, 38(3):377–393, 1990.
- [14] I. Y. Bar-Itzhack. REQUEST - a new recursive algorithm for attitude determination. *Proceedings of the National Technical Meeting of The Institute of Navigation*, pages 699–706, 1996.
- [15] D. Choukroun. *Novel methods for attitude determination using vector observations*. PhD thesis, Technion, 2003.
- [16] J. K. Thienel and R. M. Sanner. Hubble Space Telescope angular velocity estimation during the robotic servicing mission. *Journal of Guidance, Control, and Dynamics*, 30(1):29–34, 2007.
- [17] B. O. Sunde. Sensor modelling and attitude determination for micro-satellites. Master’s thesis, NTNU, 2005.
- [18] U. Jorgensen and J. T. Gravdahl. Observer based sliding mode attitude control: Theoretical and experimental results. *Modeling, Identification and Control*, 32(3):113–121, 2011.
- [19] L. Magnis and N. Petit. Angular velocity nonlinear observer from vector measurements. arXiv:1503.02870 [math.DS], 2015.
- [20] L. Landau and E. Lifchitz. *Mechanics*. MIR Moscou, 4th edition, 1982.
- [21] L. Magnis and N. Petit. Estimation of 3D rotation for a satellite from Sun sensors. *Proceedings of the 19th IFAC World Congress*, pages 10004–10011, 2014.
- [22] P. A. Ioannou and J. Sun. *Robust Adaptive Control*. Prentice-Hall, 1995.
- [23] H. K. Khalil. *Nonlinear Systems*. Prentice-Hall, 2nd edition, 1996.
- [24] H. K. Khalil. *Nonlinear Systems*. Pearson Education, 3rd edition, 2000.
- [25] The CubeSat program, Cal Poly SLO. *CubeSat Design Specification, Rev. 13*, 2014.
- [26] C. Bonnal, J.-M. Ruault, and M.-C. Desjean. Active debris removal: Recent progress and current trends. *Acta Astronautica*, 85:51–60, 2013.
- [27] D. Choukroun, I. Y. Bar-Itzhack, and Y. Oshman. Novel quaternion Kalman filter. *IEEE Transactions on Aerospace and Electronic Systems*, 42(1):174–190, 2006.
- [28] M. Schmidt, K. Ravandoor, O. Kurz, S. Busch, and K. Schilling. Attitude determination for the Pico-Satellite UWE-2. *Proceedings of the 17th IFAC World Congress*, pages 14036–14041, 2008.
- [29] R. Mahony, T. Hamel, and J. M. Pflimlin. Nonlinear complementary filters on the special orthogonal group. *IEEE Transactions on Automatic Control*, 53(5):1203–1218, 2008.
- [30] P. Martin and E. Salaün. Design and implementation of a low-cost observer-based attitude and heading reference system. *Control Engineering Practice*, 18:712–722, 2010.
- [31] J. F. Vasconcelos, C. Silvestre, and P. Oliveira. A nonlinear observer for rigid body attitude estimation using vector observations. *Proceedings of the 17th IFAC World Congress*, pages 8599–8604, 2008.

- [32] A. Tayebi, A. Roberts, and A. Benallegue. Inertial measurements based dynamic attitude estimation and velocity-free attitude stabilization. *American Control Conference*, pages 1027–1032, 2011.
- [33] H. F. Grip, T. I. Fossen, T. A. Johansen, and A. Saberi. Attitude estimation using biased gyro and vector measurements with time-varying reference vectors. *IEEE Transactions on Automatic Control*, 57(5):1332–1338, 2012.
- [34] J. Trumpf, R. Mahony, T. Hamel, and C. Lageman. Analysis of non-linear attitude observers for time-varying reference measurements. *IEEE Transactions on Automatic Control*, 57(11):2789–2800, 2012.